Active Disturbance Rejection Control of Position Control for Electrohydraulic Servo System

Lie Yu, Lei Ding, Qinlan Xie and Fangli Yu

***Abstract*—Electrohydraulic servo systems (EHSS) have been widely used in industries, especially for efficiently handling heavy loads. The purpose of this paper is to present a trajectory tracking of position control strategy which uses a closed-loop controller for EHSS system to synchronize the actual and desired positions. Generally, the PD controller is utilized extensively to control the EHSS, but the tracking performance of this approach is limited due to the nonlinear dynamics of EHSS. To achieve better control performance, the active disturbance rejection control (ADRC) is used in this paper to eliminate the nonlinear disturbance for EHSS. The simulation results show that the presented controller gains better tracking performances, such as less tracking lag and less mean absolute error (MAE), when compared with the PD controller.**

***Index Terms*—Electrohydraulic Servo Systems, Position control, PD Controller, Active Disturbance Rejection Control, Tracking Performance, Mean Absolute Error.**

I. Introduction

The driving mechanism of electrohydraulic servo systems (EHSS) has been widely used as mechanical tools in many fields of industry manufactures, including robotic systems, boring machines, aerospace areas and injection machines [1]–[3]. The extensive applications of EHSS are made due to their abilities of high load efficiency, fast response and high tracking accuracy [4].

However, it is especially hard to model the EHSS because there exist some nonlinear time-varying phenomena, such as the relationship between input current and output flow, fluid compressibility, deadband due to the internal leakage and external load [5]. Additionally, the hydraulic parameters may vary due to temperature changes and air entrapment in the hydraulic fluid. Based on the desired objectives, controller types for EHSS are classified as position control [6]–[9], velocity control [10] and force/torque control [11]–[12].

Manuscript received August 17th, 2019.

Lie Yu is with the School of Electronic and Electrical Engineering, Wuhan Textile University, Wuhan, China. (e-mail: lyu@wtu.edu.cn).

Lei Ding is with the Hubei Key Laboratory of Digital Textile Equipment, Department of Communication Engineering, Wuhan Textile University, Wuhan, China, and Hubei Key Laboratory of Medical Information Analysis & Tumor Diagnosis and Treatment, South-central University For Nationalities, Wuhan 300020, China (corresponding author to provide phone: +008618607155647; e-mail: lding@wtu.edu.cn).

Fangli Yu is with School of Information Engineering, Wuhan University of Technology, Wuhan 430070, China. (e-mail: yufangli_aewa@163.com)

Qinlan Xie is Hubei Key Laboratory of Medical Information Analysis & Tumor Diagnosis and Treatment, School of biomedical engineering, South-central University For Nationalities, Wuhan 300020, China. (e-mail: xieqinlan@126.com)

Generally, the fixed PD controller is widely utilized due to its ease of design, simple control structure and low cost. Nevertheless, the fixed PD controller is totally independent of the mathematical model of control systems. To achieve higher control accuracy, this paper utilized the active disturbance rejection control (ADRC) to improve the control effect for EHSS. Z. J. Yang et al., presented an error-based active control law based on ADRC for the transonic flutter suppression of a three dimensional elastic wing [13]. The extended state observer (ESO) provided the observed output signal and the observed total disturbance signal. The observed output signal obtained via the ESO was enabled to design a feedback control law for adjusting the output errors, while the observed total disturbance signal linearized the controlled system and guaranteed the anti-interference of the proposed controller. X. P. Geng et al., proposed a generalized predictor based control scheme to improve the system performance for non-minimum phase systems using set-point tracking and ADRC [14]. A model-based ESO was designed to estimate the system states simultaneously and disturbances through a generalized predictor to estimate the system output without time delay. L. Ren et al., proposed the ADRC with actuator saturation to reduce the load on a wind turbine drive chain [15]. A tracking differentiator was designed to estimate the error of the torsional vibration angle of the control system, while an ESO was used to estimate the strong non-linearity disturbance compensated by a linear controller in real time. S. Chen et al., presented the analytical design of ADRC with matched time delay for first-order nonlinear uncertain systems with delay [16]. As the conditions of stabilizing the closed-loop system were figured out in the form of parameters' explicit sets, the tuning laws of ADRC could be obtained directly and depicted intuitively in engineering practice.

In this paper, the paper presented the ADRC to improve the control effect for EHSS. The ESO provides the observed output signal of actual position of load, and the observed total disturbance signal consisting of linear parameter uncertainty and unmodeled dynamics. A feedback control law is used to adaptively adjust the output errors, while the disturbance signal linearizes the controlled system and guarantees the anti-interference of the proposed controller. The simulation results show that the presented ADRC provides less tracking lag and less mean absolute error (MAE) than the traditional PD controller.

II. Modeling of the Electrohydraulic Servo Systems

As pictured in Fig. 1, the EHSS mainly consists of a hydraulic and a servo valve. Based on the pressure equation, the system dynamics could be built in the following.

$$\ddot{y} = \frac{F_L - F_f}{m} \tag{1}$$

where F_L is the driving force to make load move, F_f is the frictional force which hinders the load to move, and m is the mass of load. As this paper is based on simulation, the F_f is set to be zero. In actual system, F_f should be compensated. The driving force generated by EHSS can be considered according to pressure equation.

$$F_L = P_1 A_{p1} - P_2 A_{p2} \tag{2}$$

where P_1 is the head-side pressure, P_2 is the rod-side pressure, A_{p1} is the head-side area and A_{p2} is the rod-side area.

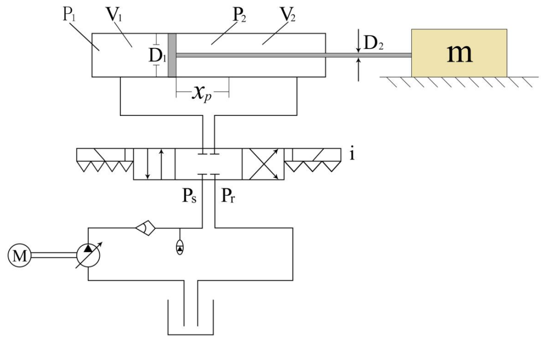

Fig. 1. Schematic Diagram of the Electrohydraulic Servo System

When the bore diameter D_1 and the rod diameter D_2 are acquired, the A_{p1} and A_{p2} can be modeled and figured out through the following formulas.

$$\begin{cases} A_{p1} = \dfrac{\pi D_1^2}{4} \\ A_{p2} = \dfrac{\pi (D_1^2 - D_2^2)}{4} \end{cases} \tag{3}$$

Based on the continuity equation presented by H. E. Merritt [16], the pressure dynamics in actuator chambers can be described as the following equations by neglecting the external leakage [17]-[18].

$$\begin{cases} \dot{P}_1 = \dfrac{\beta}{V_1}(-A_{p1} v_p - C_t P_L + Q_1) \\ \dot{P}_2 = \dfrac{\beta}{V_2}(A_{p2} v_p + C_t P_L - Q_2) \end{cases} \tag{4}$$

where $V_1 = V_0 + A_{p1} x_p$ and $V_2 = V_0 - A_{p1} x_p$ are the control volumes of the head-side and rod-side chambers, respectively. In addition, V_0 is chamber volume such that at $x_p = 0$, $V_1 = V_2 = V_0$, and x_p is displacement of the load; β is the effective bulk modulus; C_t is the coefficient of the internal leakage of the actuator due to the pressure; $P_L = P_1 - P_2$ is the load pressure of the dynamic actuator; Q_1 is the supplied flow rate to the forward chamber, while Q_2 is the return flow rate of the return chamber. Q_1 and Q_2 are related to the spool valve displacement of the servo-valve x_v.

$$\begin{cases} Q_1 = k_q x_v [s(x_v)\sqrt{P_s - P_1} + s(-x_v)\sqrt{P_1 - P_r}] \\ Q_2 = k_q x_v [s(x_v)\sqrt{P_2 - P_r} + s(-x_v)\sqrt{P_s - P_1}] \end{cases} \tag{5}$$

where P_s is the supply pressure of the fluid and P_r is the return pressure. On the other hand, k_q is the valve discharge gain which can be written as

$$k_q = C_d w \sqrt{\frac{2}{\rho}} \tag{6}$$

where C_d is the discharge coefficient, w is the spool valve area gradient and ρ is the density of hydraulic oil. Besides, the function $s(x_v)$ in Eq. (4) is defined as

$$s(x_v) = \begin{cases} 1, & x_v \geq 0 \\ 0, & x_v < 0 \end{cases} \tag{7}$$

As a high-response servo valve is used to control the hydraulic, it can be assumed that the current applied to the servo valve is directly proportional to the spool position. Their relationship can be described as

$$x_v = k_c i \tag{8}$$

where k_c is the positive electrical constant to the servo valve. As referred to the Eq. (6), the function $s(x_v)$ can be equivalent to the following formula.

$$s(x_v) = s(i) \tag{9}$$

Then, the $s(x_v)$ can be replaced by $s(i)$ such that the Eq. (4) can be rewritten as

$$\begin{cases} Q_1 = k_q k_c R_1 i \\ Q_2 = k_q k_c R_2 i \end{cases} \tag{10}$$

Additionally, the R_1 and R_2 defined in Eq. (9) are presented as

$$\begin{cases} R_1 = s(i)\sqrt{P_s - P_1} + s(-i)\sqrt{P_1 - P_r} \\ R_2 = s(i)\sqrt{P_2 - P_r} + s(-i)\sqrt{P_s - P_2} \end{cases} \tag{11}$$

In practical working conditions, both the P_1 and P_2 are needed to be bounded by P_s and P_r, which can be described that $0 < P_r < P_1 < P_s$ and $0 < P_r < P_2 < P_s$. For simulation, P_L should be bounded by P_s such that $-P_s < P_L < P_s$. This EHSS model had been successfully tested in [19]-[20], and proved to act as an actuation system to drive the load.

III. Controller Design

As the aim is to evaluate the position tracking performance for EHSS, the desired position should be acquired prior to the controller design. In Equation (1), the twice derivative of the actuated position y is computed. However, the desired position y_d for test purpose is set to be a sinusoidal signal which can be described as

$$y_d = \frac{\pi}{4}\sin(2\pi t) \tag{12}$$

After that, the controller design can be made at a sampling frequency of f_s=1000Hz to examine the behavior of the EHSS. For comparison, the fixed PD controller is selected to test the control effect of the EHSS.

A. Design of the Fixed PD Controller

Generally, the fixed PD controller is widely used due to its simple control structure, ease of design and low cost. The fixed PD controller is selected as shown in Fig. 2, and can be constructed as follows.

$$i(t) = K_p e(t) + K_d \frac{de(t)}{dt} \tag{13}$$

where K_p and K_d are the proportional and differential gains, respectively. Moreover, $e(t) = y_d(t) - y(t)$ is the error between the desired position and actuated position.

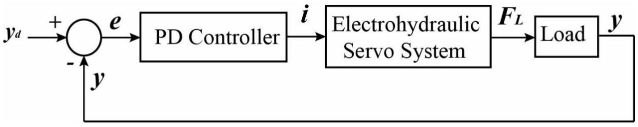

Fig. 2. Block diagram of PD controller

B. Design of the ADRC controller

In order to achieve accurate control, the system dynamic should be built completely. As the desired position y_d (as seen in Equation (12)) is given, $\dot{y}_d$ and $\ddot{y}_d$ could be figured out using the first and second derivative of y_d, respectively. However, $\dot{y}_d$ and $\ddot{y}_d$ can't be always obtained through differential mode. For ADRC, a transition process is arranged for the desired position to convert the error signal into a smooth signal to avoid the over saturation for the system output. As a result, this transition process could be expressed through an observer in the following.

$$\begin{cases} \dot{v}_1 = v_2 \\ \dot{v}_2 = -k_1(v_1 - y_d) - k_2 v_2 \\ y_d = v_1 \end{cases} \tag{14}$$

Where $\dot{y}_d = \dot{v}_1$ and $\ddot{y}_d = \ddot{v}_2$. k_1 and k_2 are the observer gains to ensure convergence of the error between v_1 and y_d to be zero.

For actual EHSS, one of the main problem is to deal with the disturbances such as unmodeled dynamics and parameter uncertainties. If the system disturbance dynamics could be measured or built, accurate control could be easily realized. In this paper, the EHSS system could be considered as a single-input single-output (SISO) system that the current (i.e., i) is the input and the position (i.e., y) is the output. The mathematical expressions between i and y are presented from Equation (1) to Equation (13) in detail. Then, through separating the controllers from states and setting disturbances produced by nonlinear disturbance to the EHSS, the model of y is rewritten by the following time-domain expressions.

$$\begin{cases} \dot{x}_1 = x_2 \\ \dot{x}_2 = b_0 i + x_3 \\ f_b = x_3 \\ y = x_1 \end{cases} \tag{15}$$

where y, $\dot{y}$ and f_b are treated as the new states x_1, x_2 and x_3 of the system, and x_3 is assumed as continuous. Meanwhile, f_b is the nonlinear disturbance, and b_0 is the amplification coefficient of i. Meanwhile, the acquisition of b_0 could be gained from experimental analysis.

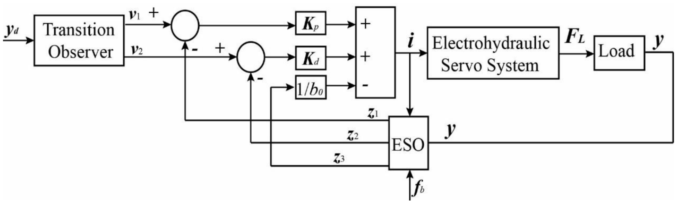

Fig. 3. Block diagram of ADRC controller

To accomplish accurate control for EHSS with nonlinear disturbances, an ADRC technology is designed. The block diagram of ADRC is depicted in Fig. 3. The key to ADRC is to design an extended state observer (ESO) to estimate both the system states and disturbance. As a result, a state observer could be used to estimate the system states and the disturbance (f_b). Let z_3 be the estimation of f_b, then the ESO could be designed using a linear structure, which is described in the following.

$$\begin{cases} \dot{z}_1 = z_2 - \beta_1(z_1 - y) \\ \dot{z}_2 = z_3 - \beta_2(z_1 - y) + b_0 i \\ \dot{z}_3 = -\beta_3(z_1 - y) \\ y = z_1 \end{cases} \tag{16}$$

where z_1, z_2 and z_3 denote the real-time estimation states of x_1, x_2 and x_3, respectively. β_i ($1 \le i \le 3$) is a positive parameter and should be designed such that z_1 tracks x_1, z_2 tracks x_2, and z_3 tracks x_3. Finally, a linear error feedback control law in the proposed control scheme is designed as follows.

$$\begin{cases} i = u_0 - \dfrac{z_3}{b0} \\ u_0 = K_{p2}(v_1 - z_1) + K_{d2}(v_2 - z_2) \end{cases} \tag{17}$$

where K_{p2} and K_{d2} are the proportional and differential gains, respectively. As reported in the literature, the ADRC has been proved to achieve successes in several common industrial problems [14-16].

IV. Simulation Results

A. Selection of System Parameters

In this section, the simulation results are stated to describe the effectiveness and superiority of ADRC compared to the fixed PD controller. For simulation, a sinusoidal signal is given as mentioned in Equation (12). while the disturbance is given as follows.

$$f_b = 0.01\sin(10\pi t) \tag{18}$$

Then, the idea in this paper has been simulated via Matlab. The parameters of EHSS are listed in Table I. The gains of the PD controller are chosen using Ziegler-Nichols method. As a result, optimum gains of K_{p1}=2 and K_{d1}=0.06 are used for the PD controller.

To realize precise control and made the EHSS stable, the parameters of ADRC are optimized and listed in Table II. Fig. 4 shows the simulation effects of ADRC. The effect of tracking signals between v_1 and z_1 is shown in Fig. 4 (a), while v_1 is the estimation of y_d, and z_1 is the estimation of y. It could be clearly seen that v_1 tracks z_1 perfectly. Similarly, Fig. 4 (b) demonstrates the performance of v_2 tracking z_2, while v_2 is the estimation of $\dot{y}_d$, and z_2 is the estimation of $\dot{y}$. As depicted in Fig. 4(b), the tracking effect is extremely great, while it takes a little time to realize full velocity tracking at the initial stage. Meanwhile, Fig. 4(c) shows the effect of tracking signals between f_b and z_3, while z_3 is the estimation of f_b. The tracking effect is relatively ideal as there exists time delay between f_b and z_3.

The simulation results in Fig. (4) demonstrate that the presented ESO has good performance in state estimation. The results prove to be reliable, and it is confidential to achieve better position and velocity tracking effects.

As shown in Fig. 5(a) and (b), the ADRC controller possess 1 ms lag, which is smaller than the PD controller (Lag=2ms). Moreover, the ADRC controller obtains smaller MAE (12.37 mm) when compared to the PD controller (MAE=12.58 mm). In order to show the comparison effect more clearly, Fig. 5(c) and (d) depict the control performance in relative short time. To augment the control performance, the error between the actual position and the desired position is calculated and demonstrated in Fig. 6. Obviously, the tracking error of the ADRC controller is smaller than that of the PD controller. To sum up, the control effect of the ADRC controller gives better performance compared with the PD controller.

TABLE I
SYSTEM PARAMETERS

Name	Symbol	Unit	value
Load mass	m	kg	7
Acceleration due to gravity	g	m/s^2	9.81
Head-side area	A_{p1}	m^2	1.77×10^{-4}
Rod-side area	A_{p2}	m^2	1.57×10^{-4}
Bore diameter	D_1	m	0.015
Rod diameter	D_2	m	0.005
Chamber volume	$V0$	m^3	1.15×10^{-4}
Effective bulk modulus	β	Pa	2×10^7
Coefficient of the total internal leakage	C_t	$m^5N^{-1}s^{-1}$	8×10^{-12}
Discharge coefficient	C_d	—	0.61
Spool valve area	w	m^2	9.59×10^{-3}
Valve discharge gain	k_q	m^2s^{-1}	2.87×10^{-4}
Supply pressure of the fluid	P_s	Pa	2×10^6
Return pressure	P_r	Pa	0.5×10^5
Density of hydraulic oil	ρ	$Kg.m^{-3}$	830
Electrical constant	k_c	$m^3s^{-1}Pa^{-1}$	1.38×10^{-4}

TABLE II
PARAMETERS FOR ADRC

Symbol	Value	Symbol	Value
b_0	1	β_1	300
k_1	1000000	β_2	30000
k_2	2000	β_3	1000000
K_{p2}	2500	K_{d2}	100

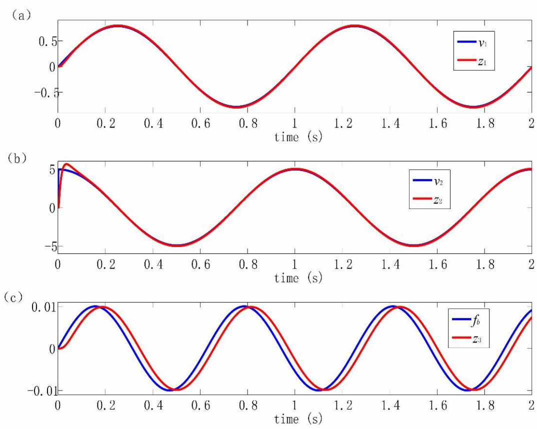

Fig. 4. Tracking effect of ADRC.

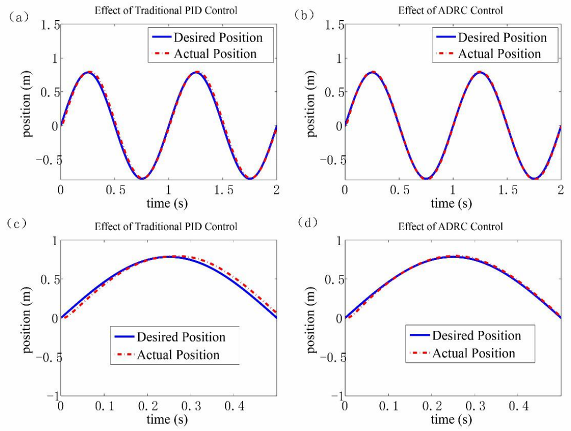

Fig. 5. Comparison of position tracking between ADRC and PD controller.

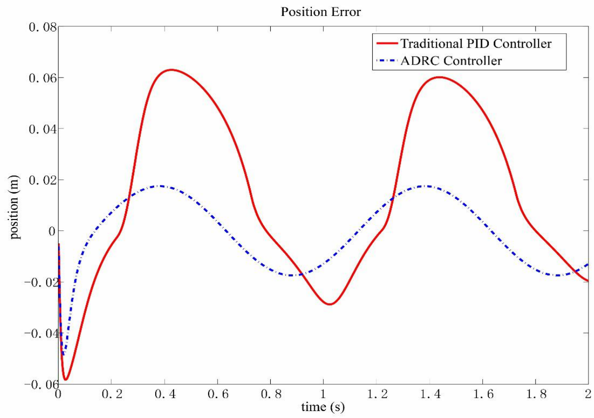

Fig. 6. Comparison of tracking error between ADRC and PD controller.

V. CONCLUSION

The mathematical model of the EHSS is built, simulated and tested successfully at the MATLAB platform. The approach to controlling the EHSS for position tracking is original for handling the load precisely. The EHSS can provide the force to make the load movement as expected due to the modeling of EHSS dynamics. Moreover, this paper has presented the ADRC controller to improve the control performance of EHSS. The simulation results show that the ADRC controller receives better performance compared with the fixed PD controller in terms of position tracking. The conclusion can be drew that the ADRC controller has given improved results when compared with the PD controllers.

VI. ACKNOWLEDGMENTS:

This work is supported by the National Natural Science Foundation of China "Research on gait detection and recognition technology of Parkinson's disease based on all-fiber composite sensors " under Grant 61903280, and Hubei Key Laboratory of Medical Information Analysis & Tumor Diagnosis and Treatment Open fund “Research on the pH detection technology of breast cancer foci edge based on micro-nano fiber composite sensor”.

This work was supported by the National Key R&D Program of China "The study on Load-bearing and Moving Support Exoskeleton Robot Key Technology and Typical Application " (2017YFB1300502)

REFERENCE

[1] J. K. Si, H. C. Feng, L. W. Ai, Y. H. Hu, "Design and Analysis of a 2-DOF Split-Stator Induction Motor", IEEE Transaction on energy conversion, vol. 30, no. 3, pp. 1200-1208, 2015.

[2] K. J. Meessen, J. J. H. Paulides, and E. A. Lomonova, "Analysis and design considerations of a 2-DOF rotary-linear actuator", in Proc. IEEE Int. Elect. Mach. Drives Conf., pp. 336–341, 2011.

[3] P. Bolognesi, "A novel rotary-linear permanent magnets synchronous machine using common active parts", in Proc. 15th IEEE Mediterranean Electrotech. Conf., pp. 1179–1183, 2010.

[4] J. C. Gao and P. D. Wu, "A fuzzy neural network controller in the electrohydraulic position control system", IEEE international conference on intelligent systems, October 28-31; Beijing, China, 1997.

[5] C. L. Hwang, "Neural-Network-Based Variable Structure Control of Electrohydraulic Servosystems Subject to huge uncertainties without persistent excitation", IEEE/ASME Transactions on mechatronics, Vol. 4, NO. 1, pp. 50-59.

[6] T. L. Chern and Y. C. Wu, "An optimal variable structure control with integral compensation for electrohydraulic position servo control systems", IEEE transaction on industrial electronics., vol. 39, no. 5, pp. 460-463, 1992.

[7] Q. P. Ha, Q. Nguyen, D. C. Rye and H. F. Durrant-Whyte, "Sliding mode control with fuzzy tuning for eletrohydraulic position servo system", 1998 second international conference on knowledge-based intelligent electronic system, April, 1998.

[8] P. Phakamach and C. Akkaraphong, "An optimal feedforward integral variable structure controller for the electrohydraulic position servo control systems", TENCON 2004. 2004 IEEE Region 10 Conference, Vol. 4, pp.459-462, 2004.

[9] E. Deticek, "An intelligent position control of electrohydraulic drive using hybrid fuzzy control structure", Proceedings of the IEEE International Symposium on Industrial Electronics., vol.3, pp. 1008-1013, 1999.

[10] G. Hasanifard, M. H. Zarif and A. A. Ghareveisi, "Nonlinear robust backstepping control of an electrohydraulic velocity servo system", Mediterranean conference on control and automation, July, 2007.

[11] S. Tafazoli, C. W. de Silva and P. D. Lawrence, "Tracking control of an elechydraulic manipulator in the presence of friction", IEEE Transactions on control system technology, May, 1998.

[12] S. Tafazoli, C. W. de Silva and P. D. Lawrence, "Friction estimation in a planar electrohydraulic manipulator", Proceedings of the American control conferences, Seatle, American, June. pp. 401-411, 1995.

[13] Z. J. Yang, R. Huang, Y. H. Zhao, H. Y. Hu, "Transonic flutter suppression for a three-dimensional elastic wing via active disturbance rejection control", Journal of Sound and Vibration, pp. 168-187, 2019.

[14] X. P. Geng, H. L. Hao, T. Liu, C. Q. Zhong, "Generalized predictor based active disturbance rejection control for non-minimum phase systems", ISA Transactions, pp. 34-45, 2019.

[15] L. Ren, C. H. Mao, Z. Y Song, F. C Liu, "Study on active disturbance rejection control with actuator saturation to reduce the load of a driving chain in wind turbines", Renewable Energy, pp. 268-274, 2019.

[16] H. E. Merritt, "Hydraulic control systems", John Wiley & Sons, (1967), New York.

[17] J. Y. Yao, Z. X. Jiao and S. S. Han, "Friction compensation for low velocity control of hydraulic flight motion simulator: A simple adaptive robust approach", Chinese Journal of Aeronautics., pp. 814-822, 2013.

[18] J. Y. Yao, Z. X. Jiao and B. YAO, "Robust Control for Static Loading of Electro-hydraulic Load Simulator with Friction Compensation", Chinese Journal of Aeronautics., pp.954-962, 2012.

[19] J. Zhang, L. Yu and L. Ding, "Velocity Feedback Control of Swing Phase for 2-DoF Robotic Leg Driven by Electro-hydraulic Servo System", Engineering Letters., pp.378-383, 2016.

[20] J. Zhang, L. Yu, J. Tang and L. Ding, "Dual Surface Sliding Mode Controller of Torque Tracking for 2-DOF Robotic Arm Driven by Electrohydraulic Servo System", Engineering Letters., pp.69-75, 2018.